Structures of α-Type Ions Formed in the 157 nm Photodissociation of Singly-Charged Peptide Ions

Liangyi Zhang, Weidong Cui, Matthew S. Thompson, and James P. Reilly
Department of Chemistry, Indiana University, Bloomington, Indiana, USA

One hundred fifty-seven nm photodissociation of singly-charged peptide ions induces the cleavage of α-carbon to carbonyl-carbon bonds along the backbone. $a_n + 1$ radical ions are observed as the primary photolysis products of peptides with N-terminal arginines in a linear ion trap mass spectrometer. The radical elimination pathways undertaken by the $a_n + 1$ radical ions to form more stable even-electron species are studied in hydrogen-deuterium (H/D) exchange experiments. Two types of a_n ions along with d-type ions are observed as secondary elimination products. The relative abundance of each depends on the C-terminal residue of the radical fragment ion. (J Am Soc Mass Spectrom 2006, 17, 1315–1321) © 2006 American Society for Mass Spectrometry

One hundred fifty-seven nm photodissociation of singly-charged peptide ions has previously been studied in a tandem time-of-flight (TOF) instrument with a vacuum matrix-assisted laser desorption/ionization (MALDI) source [1, 2]. We believe that the ultraviolet light homolytically photolyzes the backbone bond between α- and carbonyl-carbon atoms, resulting in two primary radical products: one ion and one neutral radical. As shown in Scheme **1**, when the charge is located at the peptide N-terminus, an $a_n + 1$ radical ion and neutral radical are produced. Alternatively an $x_n + 1$ radical ion along with a neutral radical is generated when the charge is at the C-terminus [1].

These primary radical ion products further undergo a secondary radical elimination, forming a- or x-type ions by eliminating a hydrogen atom, or d-, v-, and w-type satellite ions by eliminating part of the side-chain [2]. These secondary fragmentation processes are energetically accessible because 157 nm photons inject 3 to 4 eV more than that needed to cleave peptide backbone bonds. Because arginine is the most basic residue, it is assumed that it will sequester a single proton charge [3]. Therefore, 157 nm photodissociation spectra of singly-charged C-terminal arginine-containing peptides are dominated by C-terminal fragments such as x, v- and w-type ions, while peptides with N-terminal arginines yield abundant a- and some d-type ions [1, 2]. In addition, since absorbing chromophores are uniformly distributed over the length of peptides, cleavage of all α- and carbonyl-carbon bonds along the backbone is observed, resulting in excellent sequence coverage.

Singly-charged peptide ions generated by electrospray ionization (ESI) have also been photodissociated in a linear ion trap and similar fragment ions were observed [4]. ESI generated ions are much "cooler" than those produced by MALDI [5]. The similar photodissociation patterns indicate that the internal excitation deposited by 157 nm light establishes the observed fragmentation pathways. Interestingly, since the 10 ms scanning time of the ion trap is much longer than the 1 μs time between photolysis and ion acceleration in the tandem-TOF apparatus, some slow secondary processes appear to be enhanced in the trap [4]. Besides these fundamental differences, the photodissociation experiment in the ion trap offers some unique advantages over the tandem TOF study. First, the linear ion trap has a mass isolation window of 0.4 Da, making it able to isolate the monoisotopic component from the precursor isotope distribution. This simplifies tandem mass spectra and decreases the spectral overlap. Secondly, MS^n can be performed in the ion trap for the further identification of product ions, which facilitates the interpretation of ambiguous fragment peaks. These features make the linear ion trap a very powerful tool for investigating 157 nm peptide photodissociation.

In low-energy collision-induced dissociation (CID) processes, a-type ions are believed to be produced from b-type ions with a neutral loss of carbon monoxide [6, 7]. A proposed structure for a-type ions has an N=C bond on the backbone with the charge located on this tertiary nitrogen atom [6, 8]. In high-energy CID, a-type ions may arise from $a_n + 1$ intermediate ions (1 Da heavier than the normal a-type ions) since $a_n + 1$ radical ions are observed and these can fragment into a- and d-type ions [9]. Through elimination of a side-chain β-hydrogen atom from the radical ions, an alternative structure for a-type ions having a $C_\alpha = C_\beta$ bond on the side-chain of terminal residues was proposed [9].

In previous photodissociation experiments with the MALDI tandem-TOF apparatus, we observed relatively few $a_n + 1$ fragment ions and all of these had small masses [2]. Their abundance was hard to quantitatively evaluate since they overlap with the ^{13}C component of their a-type

Published online July 18, 2006

Address reprint requests to Professor J. P. Reilly, Department of Chemistry, Indiana University, Chemistry Building, 800 E. Kirkwood Ave., Bloomington, IN 47405, USA. E-mail: reilly@indiana.edu

1044-0305/06/$32.00
doi:10.1016/j.jasms.2006.06.007

Received April 20, 2006
Revised June 11, 2006
Accepted June 12, 2006

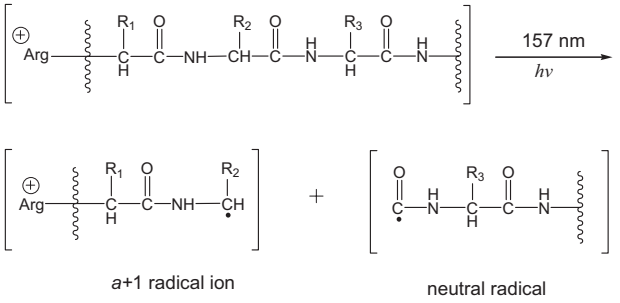

Scheme 1

counterparts. Both residual energy from the MALDI process [10, 11] and that contributed by the 157 nm light excite these radical ions, and enable them to decompose into even-electron a- and d-species through a radical elimination [2]. In the course of forming a-type ions, two different types of hydrogen atoms can be eliminated: the backbone amide hydrogen and side-chain β-carbon hydrogen. These pathways lead to different product ions. If the a-type ion structures can be established, the above two pathways can be distinguished.

Hydrogen/deuterium (H/D) exchange mass spectrometry has been widely applied to investigate biomolecular folding and conformational changes in solution and in the gas phase [12, 13]. Exchangeable hydrogen atoms are present on the peptide backbone and some side-chains. Because backbone amide hydrogen atoms are exchangeable but side-chain β-hydrogen atoms are not, the hydrogen elimination sites involved in 157 nm photodissociation experiments can be identified.

The present photodissociation work involves singly-charged peptides generated in ESI linear ion trap and MALDI tandem-TOF experiments. H/D exchange reactions enable the observation of two types of a-ions along with d-type ions. The dependence of these secondary ions on a fragment's terminal residue is elucidated.

Experimental

Materials

Peptides RPPGFSP and RYLGYLE were purchased from Sigma (St. Louis, MO). All other N-terminal arginine peptides were synthesized by Sigma Genosys (The Woodlands, TX). Deuterium oxide (D_2O) was supplied by Cambridge Isotope Laboratories, Inc. (Andover, MA). Methanol (MeOH) was obtained from Mallinckrodt Baker, Inc. (Phillipsburg, NJ). Acetonitrile (ACN) was purchased from EMD Chemicals, Inc. (Gibbstown, NJ). Formic acid (FA) was obtained from Fluka Chemika GmbH (Buchs, Switzerland). Trifluoroacetic acid-d (TFA-d) and matrix of α-cyano-4-hydroxycinnamic acid (CHCA) were bought from Sigma.

H/D Exchange of Peptides

For ESI experiments deuterated acidic Solvent A (50%D_2O, 50% ACN and 0.1% FA) was first made in the dry nitrogen glove bag. All peptides were aliquotted first and then dried with a Speed Vac. These dry peptides were resuspended into Solvent A to make 1 μM concentration solutions for electrospray. The ESI source chamber was purged with dry nitrogen. Before each experiment, the sample inlet line was flushed with D_2O for 20 min.

Photodissociation in the ESI Ion Trap and MALDI Tandem-TOF

An LTQ linear ion trap instrument (Thermo Electron, San Jose, CA) was used for these experiments. Photodissociation in the LTQ was set up as in our previous paper [4]. Briefly, the 157 nm vacuum ultraviolet (VUV) laser was introduced axially into the trap from its back side. During experiments, MS/MS mode was chosen and the excitation energy set to 0 and, therefore, no CID took place. Ions were injected into the trap and the ^{12}C component of the isotope clusters in the precursor ions was isolated for photodissociation. An F_2 laser (EX100HF-60, GAM Laser, Orlando, FL) was triggered by the activation pulse, producing 40 μJ of light in a 10 ns pulse to dissociate the peptide ions. All the product ions were scanned out to the LTQ detector as in its normal operating mode.

MALDI tandem mass spectrometry was also performed on our home-built TOF-TOF apparatus [1, 2]. Singly charged peptide ions generated by MALDI were accelerated into the first time-of-flight drift region and then separated based on *m/z*. An ion gate selected precursor ions with a mass band of about 10 Da. The 157 nm light then dissociated these precursor ions. The fragment ions were reaccelerated into a reflectron mass analyzer and then detected. Alternate shots without the photodissociation light were taken to record postsource decay (PSD) spectra. However PSD ion products did not overlap with photofragment peaks in this study and, therefore, it was not necessary to subtract them away as background.

Results and Discussion

a_n + 1 Radical Ions

In previous experiments using the MALDI tandem-TOF apparatus, a_n + 1 radical ions were observed [2]. More examples of peptides photodissociated in the MALDI tandem-TOF instrument are now presented; results are then compared with ion trap data.

Figure 1a shows the 157 nm photodissociation spectrum of peptide RPPGFSP obtained with the MALDI tandem-TOF. Expanded sections of this spectrum appear in Figure 1b. Dashed lines represent calculated isotope distributions and solid lines indicate experimental data. For a_3, a_4, and a_5 ion fragments, the a_n + 1 peaks are much more intense than predicted for ^{13}C isotope contributions as previously noted [2]. However, the isotope distribution profile of a_6 is not so different from the calculated distribution, providing little evidence for the production of a_6 + 1 radical ions.

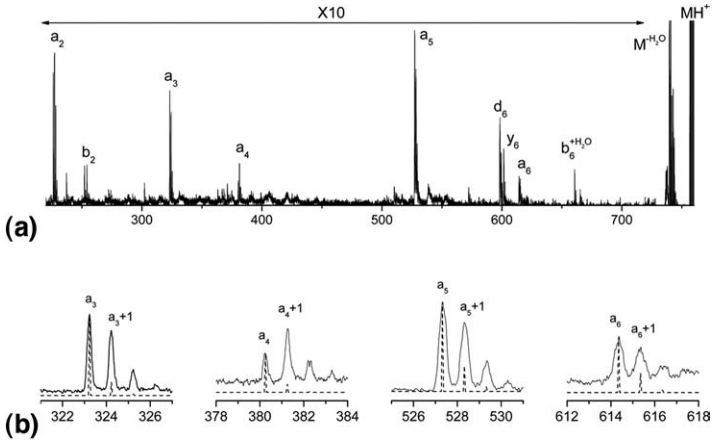

Figure 1. 157 nm photodissociation spectrum of singly-charged RPPGFSP obtained in the MALDI tandem-TOF instrument (**a**) the entire spectrum (**b**) expanded views of certain fragments. Solid lines are experimental data and dashed lines are the predicted isotopic distributions.

To improve precursor isolation, we repeated this experiment with a linear ion trap. Figure 2 displays these data. In the expanded view of the precursor ion region, only the monoisotopic peak is seen. By isolating monoisotopic peaks with the ion trap, the mass overlap between each $a_n + 1$ radical ion and ^{13}C peak of the corresponding a_n ion was removed. The absence of ^{13}C peaks is also strongly evident in the expanded views of b- and y-type ion peaks. The lack of ^{13}C contributions implies that peaks 1 Da heavier than a-type ions are entirely attributable to $a_n + 1$ radical ions. It can be seen that radical ions appear in all cases (a_3 to a_6) with rather high intensities. In fact, $a_n + 1$ radical ions were formed during cleavage of every backbone α- and carbonyl-carbon bond in 157 nm ion trap photodissociation experiments, demonstrating both their propensity to form and their stability.

Even though the fragmentation patterns observed with both instruments are similar, the relative intensities of most radical ions in the ion trap are higher than in the MALDI tandem-TOF. (The $a_6 + 1$ peak in Figures 1 and 2 is a particularly good example of this.) Since the scanning time in the ion trap is much longer than in the MALDI tandem-TOF instrument, the $a_n + 1$ radical ions have a much longer time to form, but they also must be rather stable. We have suggested that the internal excitation energy of photolytically generated radical ions drives the secondary fragmentation processes [2]. In the MALDI tandem-TOF experiments, precursor ions are thermally excited by the vacuum MALDI process and photolytically excited by laser light. However, in the ESI ion trap experiments, the internal excitation energy is mainly contributed by the light, since the electrosprayed precursor

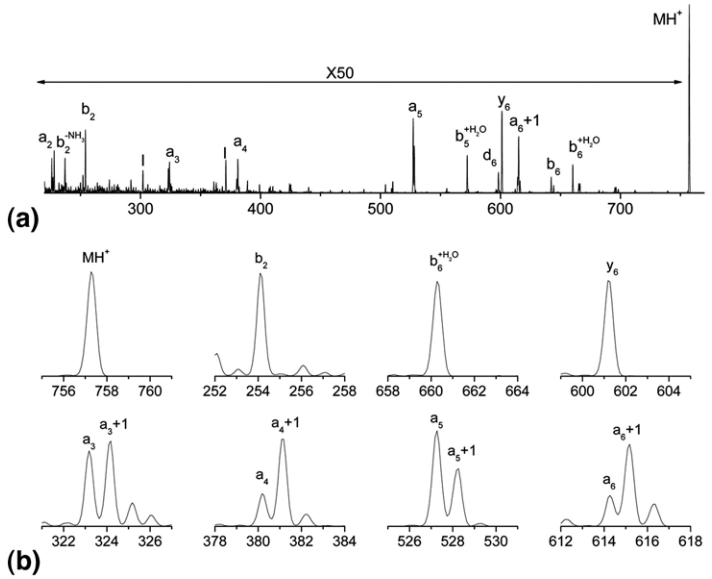

Figure 2. 157 nm Photodissociation spectrum of singly-charged RPPGFSP obtained in the linear ion trap (**a**) the entire spectrum, (**b**) expanded views of parts of the spectrum. In this experiment, monoisotopic precursor ions are isolated and irradiated.

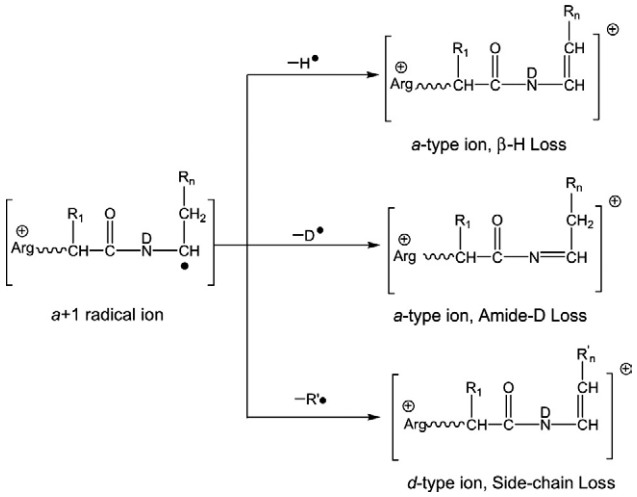

Scheme 2

ions are completely thermalized by collisions with buffer gas molecules [5]. Therefore $a_n + 1$ radical ions in MALDI tandem-TOF experiments should be much "hotter" than those generated in the ion trap.

a-Type Ion Formation Pathways

Even though $a_n + 1$ radical ions are apparently stable in the ion trap, secondary fragmentation processes also produce stable even-electron species such as a- and d-type ions. Even-electron species are produced by the elimination of a hydrogen atom or part of a side-chain.

To form a-type ions, hydrogen atoms can be eliminated from either the backbone amide or the side-chain β-carbon. Because amide hydrogen atoms are exchangeable but those bound to side-chain carbons are not, they can be differentiated through complete H/D exchange reactions as displayed in Scheme **2**.

Figure 3 shows four expanded views of a-type fragments derived from 157 nm photodissociation of singly-charged deuterated peptide RPPGFSP in the ion trap. Note that even-electron a_n ions are now labeled as $a_n + 1 - H$ or $a_n + 1 - D$ based on their mass. In the a_3 region, an $a_3 + 1 - H$ peak appears, demonstrating that only hydrogen atoms were eliminated. The intensities of other peaks are at the level of background noise. At first the a-type ion formation at proline and glycine residues were chosen as two special cases because of their unique structures. Since proline does not have backbone amide hydrogen atoms, only a hydrogen atom on the side-chain β-carbon can be eliminated from the $a_3 + 1$ radical ion, resulting in the $a_3 + 1 - H$ peak. In addition, glycine has backbone amide hydrogen atoms, but no side chain. The elimination of the backbone deuterium produces the $a_4 + 1 - D$ peak, and the absence of a_4+1-H peak is due to the lack of a β-hydrogen. These experimental observations are consistent with the structures of the proline and glycine. All other residues have both backbone amide and side-chain β-hydrogen atoms. Therefore, it is not surprising that both a_5 and a_6 ions can be generated through the elimination of either a hydrogen or deuterium atom. As shown in Scheme **2**, the loss of a backbone amide hydrogen atom generates an N=C double-bond at the backbone, while the elimination of a β-hydrogen atom results in the formation of a C_α=C_β on the side chain. Therefore, two a-type ions with different structures were produced at these amino acid residues. Furthermore, it can be seen that the loss of H appears to be favored for a_5 ions, but the two processes occur with similar likelihood for a_6 ions. These pathways will be further discussed in the following section.

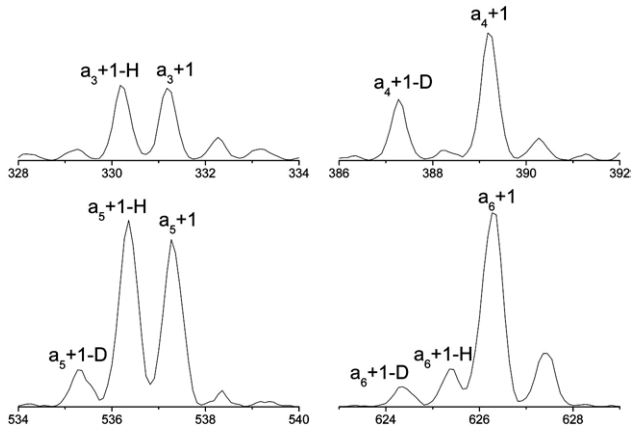

Figure 3. a-type Ion fragments in 157 nm photodissociation spectra of singly-charged deuterated RPPGFSP obtained in the ion trap.

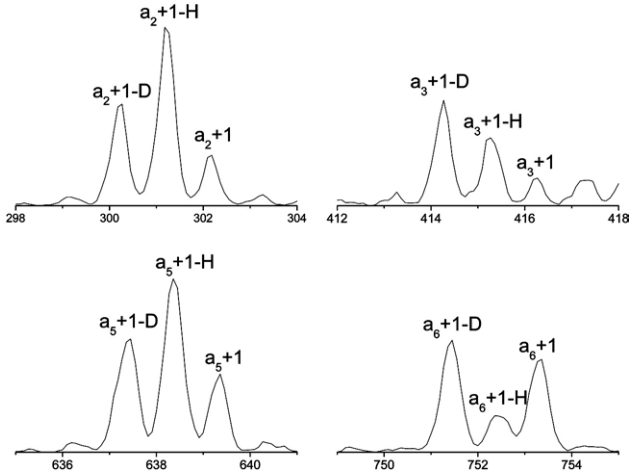

Figure 4. a-Type ion fragments in 157 nm photodissociation spectra of singly-charged deuterated RYLGYLE obtained in the ion trap.

Probability of Forming Two Types of a_n Ions

To evaluate the effect of side chain on the probability of forming a_n ions with a double-bond in each of the two possible locations, fragment ions terminated by various different amino acids were investigated. Figure 4 shows several a-type ions in ion trap photodissociation spectra of singly-charged, fully deuterated RYLGYLE. Both a_2 and a_5 fragments have C-terminal tyrosine residues and the hydrogen-elimination peaks are more intense than the deuterium-elimination peaks. For this aromatic residue, formation of a C_α=C_β bond is apparently favored, although formation of a N=C on the backbone is also quite possible.

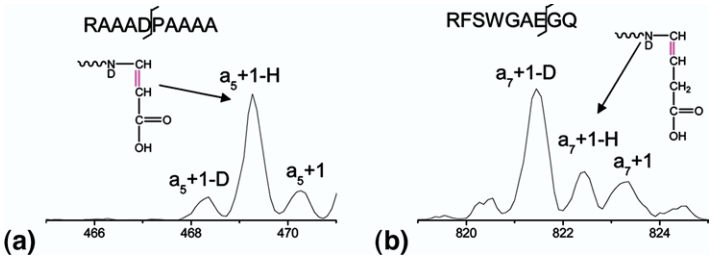

Figure 5. a-Type ion fragments (**a**) a_5 of RAAADPAAAA, (**b**) a_7 of RFSWGAEGQ, obtained from singly-charged deuterated peptide ions by 157 nm photodissociation in the ion trap.

Fragments a_3 and a_6 are terminated by a leucine residue and deuterium-elimination is the preferred process.

At 157 nm about half of the 7.9 eV photon energy is needed to break a backbone bond and the remainder is available for translational and internal excitation of the two photolysis products. The energetics of secondary processes can be roughly estimated by considering bond energies. For the backbone hydrogen elimination, N—H and N—C bonds are broken and an N=C bond is formed, leading to an overall endothermicity of 1 to 2 eV. The side chain hydrogen-elimination is similar but slightly more endothermic. The internal excitation available to the radical ions appears to be quite sufficient to drive these endothermic elimination processes. In our tandem-TOF apparatus, fragment ions have about one microsecond after light absorption before they are accelerated to undergo these processes. In the ion trap, fragment ions have several milliseconds between the time they are formed and when they are scanned out. Therefore, all three secondary fragmentation products in Scheme **2** are expected to be observed and their relative abundances may be related to their formation energetics.

Tyrosine residues have a β-carbon substituted by a conjugated aromatic ring, which makes the side chain hydrogen elimination thermally favorable since the newly formed $C_\alpha = C_\beta$ bond can conjugate with the aromatic ring. For residues with a nonaromatic side-chain like leucine and isoleucine, the double bond formed at the side chain does not lead to enhanced stability. Backbone hydrogen elimination is favored consistent with the slightly lower thermal energy needed for this process.

To further evaluate side chain conjugational effects, a-type ion formation is compared in fragments terminated by aspartate and glutamate. The side chain of glutamate is 1 CH_2 unit longer than that of aspartate, and one might expect that this difference would impact side chain conjugation. Spectra displaying a_5 of RAAADPAAAA and a_7 of RFSWGAEGQ are shown in Figure 5. While side chain elimination is clearly dominant in the aspartate case, backbone hydrogen elimination is favored at the glutamate residue. In the former case, the newly formed $C_\alpha = C_\beta$ bond is conjugated with the amide C=O bond on the side chain. This stabilizes the a-type ion, making the side chain hydrogen elimination dominant. However, the glutamate residue does not have this conjugational effect and the backbone hydrogen elimination is overwhelmingly abundant.

Fifteen different peptides with N-terminal arginine were photodissociated after complete H/D exchange and a total of 50 a-type ion fragments were observed. The intensities of $a_n + 1 - D$ and $a_n + 1 - H$ ion peaks were measured and normalized values are summarized in Table 1. The effect of all residues except cysteine, lysine, and arginine was investigated. Because peak widths were fairly constant, peak heights were used to represent ion intensities. The noise level of all photodissociation spectra was about 5 ~ 10% of a-type ion intensities. The deuterium loss peak in the proline case and the hydrogen loss peak in the glycine case were at the level of background noise and they were considered to be zero after subtracting the average background. For all other residues, both $a_n + 1 - D$ and $a_n + 1 - H$ ions were produced. From just this limited dataset, it is evident that the side-chain structure of terminal residues has a large effect on the relative intensities of the two types of a_n ions. When amino acids do not have side chain conjugational effects, $a_n + 1 - D$ ions peaks are generally more intense than $a_n + 1 - H$. Otherwise, $a_n + 1 - H$ ions are more abundant. Because glutamine stands out as the lone exception, it was further studied.

Four different glutamine-containing peptides, RGGQGG, RAAQAA, RLEQFG, and RPKPQQFFGLM-NH_2, were deuterium-labeled and photodissociated. Five a-type ion fragments terminated by glutamine were observed, as shown in Figure 6. For RGGQGG, heights of the two a-type ions are comparable. For the other peptides, the intensity of $a_n + 1 - H$ is higher than the $a_n + 1 - D$ peaks. These results do not agree with the generalization of probabilities of two types of a_n ions since glutamine is not expected to exhibit side-chain conjugation. Nevertheless, the higher intensities of hydrogen loss peaks imply that the side chain elimination from glutamine is more favorable than the backbone deuterium elimination. Possibly conformation changes of glutamine-containing ions may be affecting the energetics of these secondary fragmentation reactions since the two types of a_n ions can have significantly different gas-phase structures. Since the amide on the glutamine side chain tends to interact with the charge proton on the arginine residue [14, 15], this special intraionic interaction stabilizes the ionic structure. A double-bond on the backbone formed by deuterium elimination could easily change the backbone structure, making a less stable structure. In contrast, the structures of $a_n + 1 - H$ ions may be similar to those of $a_n + 1$ radical ions if the double-bond on the side chain does not destroy

Table 1. Probability of forming two types of a_n ions

Amino acid	Number of *a*-type ions observed	Average intensity ratio (a_n + 1-D)	Average intensity ratio (a_n + 1-H)	Standard deviation	Side-chain conjugational effect?
Proline (P)	5	0	1	-	N
Glycine (G)	3	1	0	-	N
Alanine (A)	10	0.61	0.39	0.06	N
Valine (V)	2	0.77	0.24	0.12	N
Leucine (L)	4	0.66	0.35	0.06	N
Isoleucine (I)	1	0.71	0.29	-	N
Glutamine (Q)	5	0.38	0.62	0.11	N
Glutamic acid (E)	2	0.68	0.32	0.08	N
Methionine (M)	1	0.66	0.34	-	N
Threonine (T)	1	0.59	0.41	-	N
Phenylalanine (F)	4	0.26	0.74	0.07	Y
Tyrosine (Y)	4	0.33	0.67	0.07	Y
Tryptophan (W)	1	0.29	0.71	-	Y
Histidine (H)	2	0.36	0.65	0.01	Y
Aspartic acid (D)	1	0.21	0.79	-	Y
Asparagine (N)	1	0.21	0.79	-	Y
Serine (S)	3	0.42	0.58	0.10	Y
Cysteine (C)	-	-		-	N
Lysine (K)	-	-		-	N
Arginine (R)	-	-		-	N

intraionic interactions. In summary, intraionic interactions might make side chain elimination energetically more favorable in glutamine-terminated ions. The subtle effect of secondary structure on a_n ion formation will be the subject of future modeling and experiments.

d-Type Ion Formation

As displayed in Scheme **2**, a_n + 1 radical ions can also decompose into d-type ions by eliminating part of the side-chain from the β-carbon [9]. d- and w-ions are useful for differentiating isobaric amino acids leucine and isoleucine. d-type ions were first observed by Johnson et al. in high-energy CID experiments [9]. Some d-type ions were observed in surface-induced dissociation experiments by Gu et al. later on [16]. It is of interest to compare d-type ion production by photodissociation with these earlier experiments.

Sixteen peptides with N-terminal arginine were photodissociated in the ion trap, and a total of 26 d-type ions were observed. The relative intensity ratio of a- and d-type ions is displayed in Table 2. Glycine and alanine do not form d-type ions since they do not have β-carbon substituents. Proline does not form d-type ions because of its unique five-atom

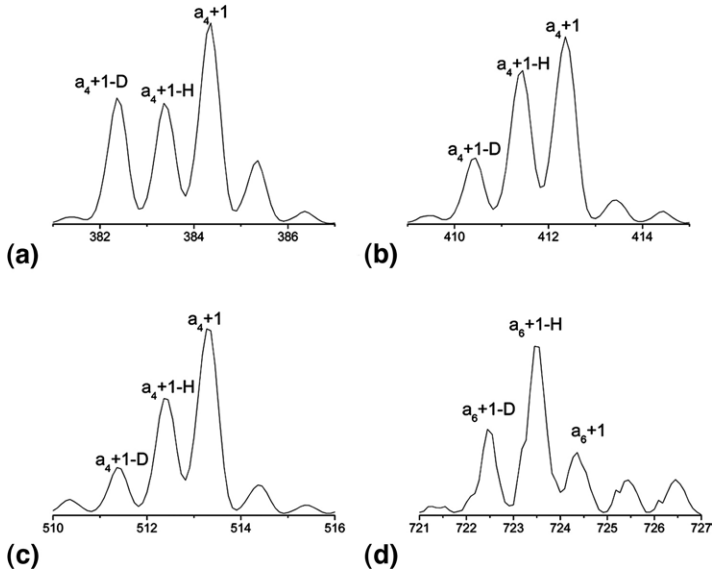

Figure 6. a-Type ion fragments (**a**) a_4 of RGGQGG, (**b**) a_4 of RAAQAA, (**c**) a_4 of RLEQFG, and (**d**) a_6 of RPKPQQFFGLM-NH_2 obtained from singly-charged deuterated peptide ions by 157 nm photodissociation in the ion trap

Table 2. *d*-Type ion formation and their intensities

Amino acid	Number of *d*-type ions observed	Average intensity ratio a_n	Average intensity ratio d_n	Standard deviation	*d*-type ion formation?
Proline (P)	0	-		-	N
Glycine (G)	0	-		-	N
Alanine (A)	0	-		-	N
Valine (V)	2	0.89	0.11	0.01	Y
Leucine (L)	8	0.66	0.34	0.14	Y
Isoleucine (I)	1	0.91	0.09	-	Y
Glutamine (Q)	5	0.41	0.59	0.09	Y
Glutamic acid (E)	2	0.60	0.41	0.11	Y
Serine (S)	3	0.62	0.38	0.13	Y
Phenylalanine (F)	0	-		-	N
Tyrosine (Y)	0	-		-	N
Tryptophan (W)	0	-		-	N
Histidine (H)	0	-		-	N
Aspartic acid (D)	1	0.40	0.60	-	Y
Asparagine (N)	1	0.48	0.52	-	Y
Methionine (M)	1	0.39	0.61	-	Y
Threonine (T)	1	0.42	0.58	-	Y
Cysteine (C)	-	-		-	-
Lysine (K)	-	-		-	-
Arginine (R)	-	-		-	-

ring side chain. Likewise, residues with aromatic side chains do not generally produce d-type ions. When these fragments were observed in high-energy peptide ion fragmentation [9], they exhibited very low intensities. This is understandable since the elimination of an aromatic group requires more energy than the elimination of a β-hydrogen or alkyl radical. However, for nonaromatic side chains, a-type and d-type ion formation is energetically comparable and both ions were observed. As expected, two different d-type ions with comparable intensities were produced at threonine and isoleucine residues. Each of these ions results from the loss of one substituent from the β-carbon on the side chain.

The production of d-type ions in 157 nm peptide photodissociation depends on the structure of fragment terminal residues, consistent with high-energy CID experiments [9]. Their propensity to be observed appears to be independent of the detailed pathway by which they are produced.

Conclusions

$a_n + 1$ radical fragment ions were observed in the ion trap after isolating the monoisotopic precursor ions. Their ubiquitous observation supports a photodissociation mechanism that involves homolytic radical cleavage. Two different a-type ion formation pathways have been distinguished by H/D exchange experiments, leading to two types of a_n ions with different structures. The relative abundances of a-type and d-type ions were also investigated. Results depend on the C-terminal residue of the ion fragment. Attempts to predict ion fragmentation patterns must take this into account.

Acknowledgments

This work has been supported by NSF grant CHE0518234, the Indiana 21st Century Fund, and the Indiana Metacyt Initiative.

References

1. Thompson, M. S.; Cui, W.; Reilly, J. P. Fragmentation of Singly Charged Peptide Ions by Photodissociation at Lambda = 157 nm. Angew. Chem. Int. Ed. **2004**, *43*, 4791–4794.
2. Cui, W.; Thompson, M. S.; Reilly, J. P. Pathways of Peptide ion Fragmentation Induced by Vacuum Ultraviolet Light. *J. Am. Soc. Mass Spectrom.* **2005**, *16*, 1384–1398.
3. Harrison, A. G. The Gas-Phase Basicities and Proton Affinities of Amino Acids and Peptides. *Mass Spectrom. Rev.* **1997,** *16*, 201–217.
4. Kim, T. Y.; Thompson, M. S.; Reilly, J. P. Peptide Photodissociation at 157 nm in a Linear Ion Trap Mass Spectrometer. *Rapid Commun. Mass Spectrom.* **2005,** *19*, 1657–1665.
5. Liere, P.; Steiner, V.; Jennings, K. R.; March, R. E.; Tabet, J. C. Influence of Ion Activation and Thermalization Effects on Reaction Rate Constants in a Quadrupole Ion Trap Mass Spectrometer. *Int. J. Mass Spectrom.* **1997,** *167*, 735–751.
6. Biemann, K. Contributions of Mass Spectrometry to Peptide and Protein Structure. *Biomed. Environ. Mass Spectrom.* **1988,** *16*, 99–111.
7. Papayannopoulos, I. A. The Interpretation of Collision-Induced Dissociation Tandem Mass-Spectrometry of Peptides. *Mass Spectrom. Rev.* **1995,** *14*, 49–73.
8. Biemann, K. Nomenclature for Peptide Fragment Ions (Positive Ions). *Methods Enzymol.* **1990,** *193*, 886–887.
9. Johnson, R. S.; Martin, S. A.; Biemann, K. Collision-Induced Fragmentation of $(M + H)^+$ Ions of Peptides Side-Chain Specific Sequence Ions. *Int. J. Mass Spectrom. Ion Processes* **1988,** *86*, 137–154.
10. Spengler, B.; Kirsch, D.; Kaufmann, R. Metastable Decay of Peptides and Proteins in Matrix-Assisted Laser-Desorption Mass Spectrometry. *Rapid Commun. Mass Spectrom.* **1991,** *5*, 198–202.
11. Spengler, B.; Kirsch, D.; Kaufmann, R. Fundamental-Aspects of Postsource Decay in Matrix-Assisted Laser Desorption Mass-Spectrometry. I. Residual Gas Effects *J. Phys. Chem.* **1992,** *96*, 9678–9684.
12. Katta, V.; Chait, B. T. Conformational -Changes in Proteins Probed by Hydrogen-Exchange Electrospray-Ionization Mass-Spectrometry. *Rapid Commun. Mass Spectrom.* **1991,** *5*, 214–217.
13. Winger, B. E.; Lightwahl, K. J.; Rockwood, A. L.; Smith, R. D. Probing Qualitative Conformation Differences of Multiply Protonated Gas-Phase Proteins Via H/D Isotope Exchange with D_2O *J. Am. Chem. Soc.* **1992,** *114*, 5897–5898.
14. Schnier, P. D.; Price, W. D.; Jockusch, R. A.; Williams, E. R. Blackbody Infrared Radiative Dissociation of Bradykinin and Its Analogues: Energetics, Dynamics, and Evidence for Salt-Bridge Structures in the Gas Phase. *J. Am. Chem. Soc.* **1996,** *118*, 7178–7189.
15. Wyttenbach, T.; Paizs, B.; Barran, P.; Breci, L.; Liu, D.; Suhai, S.; Wysocki, V. H.; Bowers, M. T. The Effect of the Initial Water of Hydration on the Energetics, Structures, and H/D Exchange Mechanism of a Family of Pentapeptides: An Experimental and Theoretical Study. *J. Am. Chem. Soc.* **2003,** *125*, 13768–13775.
16. Gu, C.; Somogyi, A.; Wysocki, V. H.; Medzihradszky, K. F. Fragmentation of Protonated Oligopeptides XLDVLQ (X=L, H, K, or R) by Surface Induced Dissociation: Additional Evidence for the "Mobile Proton" Model. Anal. Chim. Acta **1999**, *397*, 247–256.